ARTICLES

State-to-State Reactive Scattering via Real L^2 Wave Packet Propagation for Reduced Dimensionality AB + CD Reactions[†]

Sergei Skokov[‡] and Joel M. Bowman*

Department of Chemistry and Cherry L. Emerson Center for Scientific Computation,
Emory University, Atlanta, Georgia 30322

Received: June 20, 2000; In Final Form: August 24, 2000

We present a computational method for the calculation of quantum state-to-state reactive probabilities for reduced dimensionality, three degree-of-freedom, AB + CD ↔ A + BCD reactions. Our approach is based on the recently developed wave packet propagation method in real L^2 eigenstates [Skokov, S.; Bowman, J. M. *Phys. Chem. Chem. Phys.* **2000**, *2*, 495]. Here we show how the real L^2 approach can be used for the calculation of state-to-state probabilities. The "coordinate transformation problem" is relatively easily solved in the L^2-eigenstate formulation because the eigenstates used for propagation are analytical functions of the coordinates. The method is tested for the H_2 + CN ↔ H + HCN reaction for zero total angular momentum, J, using a previous potential energy surface of Sun and Bowman, who reported reduced dimensionality, time-independent calculations of state-to-state reaction probabilities. New calculations for $J > 0$ are presented using the adiabatic rotation approximation. In this approximation the L^2-eigenstates are obtained efficiently by expanding them in the basis of $J = 0$ eigenstates. Finally a test of J-shifting is done.

I. Introduction

The calculation of the full state-to-state probability matrix is perhaps the most challenging problem in reactive scattering. While thermally averaged properties can be easily (though approximately) captured within transition state theory, the calculation of state-selected and state-to-state transitions requires rigorous quantum approaches. With the progress in experimental techniques, state-selected and state-to-state probabilities for many interesting systems have become available and thus can serve as a benchmark for theoretical methods.

One of the popular tools for studying reaction dynamics is wave packet propagation.[1] The techniques that are currently used employ direct propagation of the wave packet on a grid.[2] The most widely used methods are the split-operator method[3] and the Chebyshev propagation method.[4] These methods have been augmented by damping potentials[5−7] to allow for application to reactive scattering.[8,9] The negative imaginary potential method has been successfully applied by Neuhauser, Kouri, Baer, and co-workers[6] for three-dimensional wave packet propagation. This and other approaches[10−15] reduce the size of the spatial grid and thereby greatly increase the efficiency of wave packet propagation.

In these direct propagation methods initial state-selected reaction probabilities can be easily extracted over a range of initial relative kinetic energies by the flux method applied to the reactant set of coordinates.[1] Thus, these methods are ideally suited for applications to initial state-selected experiments. However, the calculation of state-to-state probabilities presents a significant challenge for wave packet propagation methods. Reactant Jacobi coordinates have proven to be a very good choice for propagation of wave packets; however, these coordinates do not provide an efficient representation of product states, and so the accurate transformation of the wave packet between reactant and product Jacobi coordinates on a finite grid is computationally difficult. Thus, the projection of the wave packet onto the final product states, which typically has to be done at each time step, may be extremely time-consuming. A variety of approaches has been proposed to circumvent the "coordinate transformation problem". One approach is to propagate an initial wave packet in reactant coordinates and switch to product coordinates when the wave packet enters the strong interaction region.[16] The problem, however, is the significant spread of the wave packet at the time it arrives in the interaction region. Another important approach is to decouple the wave packet into the reactant and product components and carry out the propagation of independent wave packets in both sets of coordinates.[17,18] Finally, a relatively straightforward approach is to set up an initial wave packet in product coordinates, transform this wave packet to reactant coordinates, and propagate in reactant coordinates and do the flux analysis in reactant coordinates.[9] We adopt that approach here.

A second challenging problem in reactive scattering is the calculation of reaction probabilities for nonzero total angular momentum, J. Exact calculations of state-to-state reaction probabilities for $J > 0$ are extremely time-consuming, and for most systems such calculations are prohibitively expensive. (Such calculations have been done for a number of atom−

[†] Part of the special issue "William H. Miller Festschrift".

* To whom correspondence should be addressed. Email: bowman@euch4e.chem.emory.edu.

[‡] Present address: Intel Corp., 2200 Mission College Blvd., MS SC12−205, Santa Clara, CA 95052.

10.1021/jp0022151 CCC: $20.00

diatom systems containing H_2 molecules; however, not yet for any tetraatomic system.) Therefore, the development of approximate methods for the treatment of overall rotation is an important subject of gas-phase quantum dynamics.

The simplest, yet surprisingly accurate, approximation for $J > 0$ is the so-called *J*-shifting approximation.[19] In its simplest form, *J*-shifting requires exact (or approximate) reaction probabilities for $J = 0$ and knowledge of rotational constants at some reference geometry (typically the transition state) and assumes that these constants are independent of energy and *J* value. This assumption is valid for reactions with substantial barriers; however, the choice of reference geometry becomes somewhat ambiguous if the reaction proceeds via formation of a long-lived, intermediate complex. To avoid this ambiguity, or in general to determine a more accurate set of rotational constants, more sophisticated extensions of *J*-shifting have been proposed.[20−26] For complex-forming reactions, with no barrier, the position of the transition state is determined by the rotation of the molecular system and thus depends on *J* (and *K*, the body-fixed projection quantum number).[27,28]

More accurate, but still approximate $J > 0$ calculations are typically carried out within the centrifugal sudden (CS)[29,30] or adiabatic rotation (AR)[31−33] approximations. Within these approximations the computational effort for each *J* is roughly the same as for a $J = 0$ calculation. Such favorable scaling makes these calculations feasible, yet even such linear scaling becomes a burden if calculations for many *J* values are of interest.

In this paper, we present an extension and application of a wave packet propagation method that uses real L^2 eigenstates with damping. This method was described and tested for the three-dimensional D + H_2 → HD + H reaction ($J = 0$).[34] In this approach, the scattering problem is divided into two separate problems: the calculation of L^2 eigenstates and propagation of a wave packet expanded into the eigenstates. Calculation of eigenstates might be prohibitively expensive; however, if they can be obtained, the propagation for many initial states is very efficient. Therefore, this method can be an alternative to grid-based methods for the calculation of thermally averaged properties. It has been recently applied to the calculation of the thermal rate constants of O(^{3}P) + HCl reaction[35] and a reduced dimensionality description of the H_2 + diamond (111) reaction.[36] In these applications, initial state-selected reaction probabilities were calculated.

Here we extend this approach to obtain state-to-state reaction probabilities, for $J \geq 0$, based on the adiabatic rotation approximation, for reduced dimensionality AB + CD reactions. The details of this extension are given in section II. An application and test of the method is presented in section III for the previously studied H_2 + CN reaction in three degrees of freedom.[37] New results for $J > 0$ and a test of *J*-shifting are also given in that section. A summary is given in section IV.

II. Theory and Computational Methods

A. Calculation of $J = 0$ Real L^2 Eigenstates. As mentioned in the Introduction, the evaluation of real L^2 eigenstates for reactive scattering is the most challenging and time-consuming part of the calculation. Wave packet propagation via L^2 eigenstates does not depend on the method of computing eigenstates,[34] but the practical implementation does, of course, depend on the particular approach used for calculation of eigenstates.

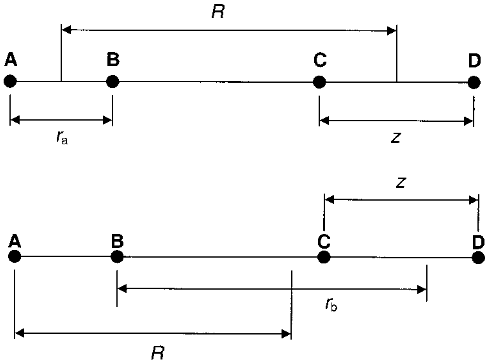

Figure 1. Jacobi coordinates for collinear AB + CD reaction in reactant (a) and product (b) arrangement.

We describe our procedure for the calculation of eigenstates for reduced dimensionality AB + CD ↔ A + BCD reactions where the CD bond is treated as a spectator mode. The present formulation closely follows the previous reduced dimensionality/adiabatic bend model of Sun and Bowman for time-independent scattering.[37] Let us denote reactant Jacobi radial coordinates as R_a, r_a, and z_a and the product Jacobi coordinates as R_b, r_b, and z_b; these coordinates are depicted in Figure 1. The $J = 0$ three degree-of-freedom Hamiltonian in reactant coordinates is given by (in atomic units)[37,38]

$$\hat{H}_{3d}^{J=0} = -\frac{1}{2\mu_{R_a}}\frac{\partial^2}{\partial {R_a}^2} - \frac{1}{2\mu_{r_a}}\frac{\partial^2}{\partial {r_a}^2} - \frac{1}{2\mu_{z_a}}\frac{\partial^2}{\partial {z_a}^2} + V_{coll}(R_a,r_a,z_a) + V_{bend} \tag{1a}$$

where V_{bend} is the adiabatic bending energy. For the collinearly dominated H_2 + CN reaction it is given in the harmonic approximation by

$$V_{bend} = (n_b + 1)\hbar\omega_n(R_a,r_a,z_a) + (m_b + 1)\hbar\omega_m(R_a,r_a,z_a) \tag{1b}$$

where n_b and m_b are the bending quantum numbers of the two doubly degenerate bends, with harmonic frequencies ω_n and ω_m, respectively. Thus, in this reduced dimensionality approach, three (radial) degrees of freedom are treated in a fully coupled fashion while the remaining three (angular) internal degrees of freedom are treated approximately by the adiabatic bend method.

The method employed to obtain the eigenfunctions of this Hamiltonian is a variation of a truncation/recoupling technique discussed in detail elsewhere.[39] In brief, the 3 degree-of-freedom eigenstates were sought in the form

$$\Psi_i^{3d} = \sum_{j,k} C_{ijk}^{3d}\Psi_j^{2d}(R_a,r_a)\phi_k(z_a) \tag{2a}$$

where

$$\Psi_j^{2d} = \sum_{l,m} C_{jlm}^{2d}\phi_l(R_a)\phi_m(r_a) \tag{2b}$$

One-dimensional eigenstates $\phi(R_a)$, $\phi(r_a)$, $\phi(z_a)$ were obtained by diagonalization of appropriate one-dimensional reference Hamiltonians. Finite matrix representations of $\hat{h}(R_a)$, $\hat{h}(r_a)$, and $\hat{h}(z_a)$ were obtained with the equally spaced DVRs of Colbert and Miller.[40] The value of radial eigenstates at any arbitrary point can be easily recovered from their DVR matrixes using the underlying DVR basis functions[40]

$$\langle x|x_i\rangle = \frac{\sin[\pi(x - x_i)/\Delta x]}{\pi(x - x_i)} \tag{3}$$

where Δx is the grid spacing. We saved DVR matrices for future coordinate transformations, while the radial eigenstates were reevaluated in potential-optimized discrete variable representation (PODVR).[41] A two-dimensional reference Hamiltonian was diagonalized in a direct-product PODVR basis of R_a and r_a. The final 3 degree-of-freedom basis, formed as the direct-product of 2-D eigenfunctions, $\Psi^{2d}(R_a,r_a)$, and 1-D eigenfunctions $\phi(z_a)$, was truncated by keeping only the n lowest energy basis functions.

B. Initial State-Selected Propagation. For a time-independent Hamiltonian, the wave packet at any time t can be expanded in terms of the eigenstates as follows (in atomic units):

$$\psi(t) = \sum_n C_n \Psi_n^{3d} e^{-iE_n t} \tag{4}$$

where

$$C_n = \langle \Psi_n^{3d} | \psi(t{=}0) \rangle \tag{5}$$

and E_n are the eigenvalues of the Hamiltonian. The initial wave packet in reactant coordinates is given by

$$\psi(R_a,r_a,z_a,t{=}0) = \left(\frac{1}{\pi\alpha^2}\right)^{1/4} e^{-ik_0R_a} e^{-(R_a-R_0)^2/2\alpha^2} \phi_\nu^{AB}(r_a)\phi_j^{CD}(z_a) \tag{6}$$

where $\phi_\nu^{BC}(r_a)$ is the initial vibrational state of AB and $\phi_j^{CD}(z_a)$ is the initial vibrational state of CD. Substituting eq 6 into eq 5 one obtains

$$C_n = \sum_{l,k} C_{nlk}^{3d} S_{kj}^z \sum_{m,p} C_{lmp}^{2d} S_m^R S_{p\nu}^r \tag{7}$$

where S_{kj}^z, S_m^R, and $S_{p\nu}^r$ are the one-dimensional overlap integrals between the initial wave packet and the one-dimensional basis functions $\phi(z_a)$, $\phi(R_a)$, and $\phi(r_a)$, respectively.

To eliminate unphysical reflections of the wave packet by the edges of grid, we use the following damping technique. Let us denote the propagated and damped wave packet at the first time step by $\psi(\Delta t)$ and $\psi^{D_1}(\Delta t) = D\psi(\Delta t)$, respectively. Here, D is a damping function, which is equal to 1 almost everywhere on the grid and decays near the grid edges;[9] we use

$$D(R_a,r_a) = \begin{bmatrix} e^{-C_d(R_a-R_d)^2}, & R_a > R_d \\ e^{-C_d(r_a-r_d)^2}, & r_a > r_d \end{bmatrix} \tag{8}$$

The damped wave packet cannot be represented by the usual expression, eq 4, for the undamped packet. However, new expansion coefficients, B_k, can be obtained in terms of a damping matrix **D** via the equation

$$B_k(\Delta t) = \sum_n D_{k,n} C_n e^{-iE_n\Delta t} \tag{9}$$

where

$$D_{k,n} = \langle \Psi_k^{3d} | \hat{D}(R_a,r_a) | \Psi_n^{3d} \rangle \tag{10}$$

The propagation to the next time step proceeds as usual, i.e.

$$\psi^{D_1}(2\Delta t) = \sum_k B_k(\Delta t) \Psi_k^{3d} e^{-iE_k\Delta t} \tag{11}$$

We damp again to get

$$\psi^{D_2}(2\Delta t) = D\sum_k B_k \Psi_k^{3d}(\Delta t) e^{-iE_k\Delta t} = \sum_l B_l \Psi_l^{3d} \tag{12}$$

where

$$B_l(2\Delta t) = \sum_k D_{l,k} B_k(\Delta t) e^{-iE_k\Delta t} \tag{13}$$

This procedure continues recursively for any number of time steps.

An explicit expression for **D** is obtained by substituting the eigenstates and damping function into eq 10, and one obtains **D** as

$$D_{k,n} = \sum_{j,r,i} C_{kji}^{3d} C_{nri}^{3d} \sum_{l,m,s,q} C_{jlm}^{2d} C_{rsq}^{2d} [D_{ls}^R + D_{mq}^r] \tag{14}$$

where D_{ls}^R and D_{mq}^r are the matrix elements of damping function in the bases of one-dimensional functions $\phi(R_a)$ and $\phi(r_a)$, respectively. Note that the damping matrix does not depend on time or choice of initial wave packet, therefore, it has to be computed only once. Also, it is clear from the form of the damping function that **D** is diagonally dominant. Numerical experiments have shown that many of the off-diagonal elements of the damping matrix can be neglected without compromising accuracy. This allows us to implement a sparse matrix multiplication algorithm, which significantly reduces the CPU effort for propagation.

To obtain the reaction probability from the initial state, the wave packet is Fourier transformed to the energy representation to obtain the scattering wave function[42−44]

$$\psi^+(E) = \lim_{T\to\infty} \frac{1}{a(E)} \int_0^T e^{iEt} \psi(t)\, dt \tag{15}$$

where

$$a(E) = -\left(\frac{4\pi\alpha^2\mu^2}{k_E^2}\right)^{1/4} e^{-\alpha^2(k_E-k_0)^2/2} \tag{16}$$

Here E is the continuous collision energy, k_E is the corresponding wavenumber, and μ is the system reduced mass for the relative translational motion. Substituting the expansion of $\psi(t)$ in terms of eigenstates into eq 15, one gets the following expression for $\psi^+(E)$:

$$\psi^+(E) = \frac{1}{a(E)} \sum_n \Psi_n^{3d} Q_n \tag{17a}$$

where

$$Q_n = \sum_k B_n(t_k) e^{iEt_k} \tag{17b}$$

Here t_k is the discrete time, and note we moved the time-independent eigenstates in front of Fourier sum. Since time and spatial variables are separable for eigenstates of a time-independent Hamiltonian, the propagation is reduced to the calculation of new coefficients via recursion (9)−(13) and accumulation of Fourier sums Q_n in eq 17b.

To obtain initial state-selected reaction probabilities we use the flux approach,[6,42,44] where the flux is obtained at a fixed value of coordinates r_a^* and R_a^*. Thus, the initial state-selected reaction probability is given by

$$P_r(E) = \frac{1}{\mu_{r_a}} \mathrm{Im}\left\langle \psi^+(E) \left| \frac{\mathrm{d}}{\mathrm{d}r_a} \psi^+(E) \right\rangle \right|_{r^*_a} = \frac{1}{a^2(E)\mu_{r_a}} \sum_{n,m} S^{3d}_{n,mm}\ \mathrm{Im}\ Q_n Q_m \quad (18)$$

where $\mathbf{S}^{3d}$ is the time-independent matrix of overlaps between eigenstates and their derivatives at fixed r^*_a value, i.e.

$$S^{3d}_{n,m} = \left\langle \Psi^{3d}_n \left| \frac{d}{dr_a} \Psi^{3d}_m \right\rangle \right|_{r^*_a} = \sum_{i,j,k,l} C^{3d}_{nik}\, C^{3d}_{mjl}\, S^{2d}_{i,j} \delta_{kl} \quad (19)$$

where the two-dimensional overlap integrals are

$$S^{2d}_{i,j} = \sum_{r,s,p,q} C^{2d}_{irs}\, C^{2d}_{jpq} \delta_{rp} \phi_s(r_a) \frac{\partial \phi_q(r_a)}{\partial r_a} \bigg|_{r^*a} \quad (20)$$

Using similar equations we also computed the nonreactive probability, $P_{nr}(E)$, at the R^*_a dividing surface and used the condition $P_r(E) + P_{nr}(E) = 1$ as a convergence check. Note that the above overlap matrices, like the damping matrix, do not depend on time or the choice of initial wave packet. Therefore, they also need to be computed only once. The total CPU effort for the computation of the damping and overlap matrices is significant and may be as much one-half of CPU effort required for the calculation of eigenstates.

C. State-to-State Propagation. For the calculation of state-to-state reaction probabilities we took advantage of the closure relation

$$P_r(E) = \sum_f P_{i\to f}(E) = \frac{1}{\mu_{r_a}}\ \mathrm{Im} \sum_f \langle \psi^+(E) | \varphi_f \rangle \langle \varphi_f | \mathrm{d}\psi^+(E)/\mathrm{d}r_a \rangle |_{r^*a} \quad (21)$$

where the summation index f is over all final product states. Since the propagation is carried out in reactant Jacobi coordinates, it is more convenient to evaluate projections of the wave packet onto the reactant states, as was mentioned in Introduction. Therefore, the initial wave packet corresponds to the final state l in product coordinates, and is given by

$$\psi(R_b,r_b,z_b;t{=}0) = \left(\frac{1}{\pi\alpha^2}\right)^{1/4} \mathrm{e}^{-ik_0R_b} \mathrm{e}^{-(R_b-R_0)^2/2\alpha^2} \Psi_l(r_b,z_b) \quad (22)$$

Here $\Psi_l(r_b,z_b)$ is the two degree-of-freedom final state of the BCD molecule (in a given adiabatic bend state). The coordinate transformation between the two sets of Jacobi coordinates is[45]

$$\begin{pmatrix} r_b \\ R_b \end{pmatrix} = \begin{pmatrix} 1 & -\dfrac{m_A}{m_{AB}} \\ \dfrac{m_{CD}}{m_{BCD}} & \dfrac{Mm_B}{m_{AB}m_{BCD}} \end{pmatrix} \begin{pmatrix} R_a \\ r_a \end{pmatrix} \text{ and } z_b = z_a \quad (23)$$

where m_A, m_B, m_C, and m_D are the masses of A, B, C, and D, respectively, M is the total mass, $m_{AB} = m_A + m_B$, $m_{BC} = m_B + m_C$, $m_{CD} = m_C + m_D$, and $m_{BCD} = m_B + m_C + m_D$. (Note that there was a typo in eq 7 of Ref 45) Similar to the work of Gray and Balint-Kurti[9] we expressed the initial wave packet on reactant grid as

$$\psi(R_a,r_a,z_a;t = 0) = \psi(\tilde{R}_b,\tilde{r}_b,\tilde{z}_b;t = 0) \quad (24)$$

where $\tilde{R}_b$, $\tilde{r}_b$, and $\tilde{z}_b$ are the values of product coordinates obtained at each grid point of reactant coordinates via eq 23. Substituting the right-hand side of eq 24 into eq 2, the expansion coefficients are obtained as three-dimensional integrals over the reactant grid in contrast to one-dimensional integrals, eq 7, for wave packets in reactant coordinates. In practice, this integration can be done over a small part of the grid, since the initial wave packet is well localized, and thus it turns out to be relatively inexpensive to do these integrals. Alternatively, one can evaluate all (about 200 in present study) one-dimensional basis functions on the product grid and substitute them into eq 2 along with wave packet from eq 22 to compute expansion coefficients. As before, the evaluation of wave packet expansion coefficients has to be done only once for each initial wave packet. Once the expansion coefficients are known, the propagation is carried in reactant coordinates through recursive relations eqs 9−14, but now the wave packet is moving from the product region into the reactant region.

Since the initial wave packet represents a particular final product state, denoted generically as f, we perform the state-to-state flux analysis at the R^*_a dividing surface by projecting the scattering wave function onto the initial states, denoted generically as i, in reactant coordinates. Thus, the forward state-to-state reaction probability $P_{i\to f}(E)$ is obtained by microscopic reversiblity from $P_{f\to i}(E)$ which is given by

$$P_{f\to i}(E) = \frac{1}{\mu_{R_a}}\ \mathrm{Im}\langle \psi^+(E) | \varphi_i \rangle \langle \varphi_i | d\psi^+(E)/\mathrm{d}R_a \rangle |_{R^*_a} \quad (25)$$

where $\varphi_i = \phi^{AB}_\nu(r_a)\phi^{CD}_j(z_a)$. In the eigenstate basis the integrals to be evaluated are of the form

$$\langle \Psi^{3d}_n | \phi^{AB}_\nu(r_a)\phi^{CD}_j(z_a) \rangle \quad \text{and} \quad \langle \phi^{AB}_\nu(r_a)\phi^{CD}_j(z_a) | \mathrm{d}\Psi^{3d}_n/\mathrm{d}R_a \rangle \quad (26)$$

The calculation of these integrals is fast and contributes negligibly to the total CPU time.

As noted previously,[34,35] an advantage of the eigenbasis approach is that the propagation of any intial wave packet is quite efficient compared to the calculation of the eigenbasis. Thus, the propagation could have been carried out in A+BCD Jacobi coordinates as easily as in the chosen AB+CD ones.

D. Propagation for J > 0. The rovibrational Hamiltonian in the adiabatic rotation approximation and with a collinear minimum energy potential surface is given by[31b]

$$\hat{H}^J_{3d} = H^{J=0}_{3d} + B(R_a,r_a,z_a)J(J + 1) \quad (27)$$

where the rotational constant B is evaluated at each grid point. The propagation in eigenstates proceeds straightforwardly (however, see below) once the eigenstates of $\hat{H}^J_{3d}$ are known. Since the rotational term in (27) is essentially a perturbation, we use the eigenstates of the $J = 0$ Hamiltonian as a basis for the calculation of $J > 0$ eigenstates. This results in a signficant saving in computational effort because the number of $J = 0$ eigenstates needed to obtain the $J > 0$ eigenstates is typically 5−10 times smaller than number of 3D basis functions used to obtain the $J = 0$ eigenbasis.

To proceed, we compute the **B**-matrix in the representation of $J = 0$ eigenstates, i.e.

$$B_{ij} = \langle \Psi^{3d,J=0}_i | B(R_a,r_a,z_a) | \Psi^{3d,J=0}_j \rangle \quad (28)$$

Then the matrix representation of $\hat{H}^J_{3d}$ for any J can be easily constructed as

$$H^J_{ij,3\mathrm{d}} = E_{i,3\mathrm{d}}\delta_{ij} + B_{ij}J(J+1) \tag{29}$$

After diagonalization of this matrix, new $J > 0$ eigenstates are related to the $J = 0$ eigenstates by

$$\Psi_i^{3\mathrm{d},J} = \sum_j U_{ij}\Psi_j^{3\mathrm{d},J=0} \tag{30}$$

where U_{ij} is the usual transformation matrix.

Once the transformation matrix is known, the calculation of expansion coefficients (eq 10), damping matrix (eq 14), and overlap matrices (eqs 19, 20, 26) amounts to a simple transformation from the old ($J = 0$) to the new ($J > 0$) representation. The only additional overhead associated with $J > 0$ propagation is the calculation of the **B**-matrix, which needs to be done once, and diagonalization of small $\mathbf{H}^J_{3\mathrm{d}}$ matrix for each J value.

There is one additional point that needs to be addressed before the above procedure can be implemented, namely the long range of the rotational potential for large values of J. This would require larger grids in the scattering coordinate than is needed for the $J = 0$ eigenbasis. To deal with this problem, we followed the approach of Gray et al.[27] Instead of using the analytical normalization factor $a(E)$ given by eq 16, we propagated a one-dimensional wave packet on an effective potential (averaged over the initial vibrational state) to a large value of R, and then calculated the normalization factor for the distorted wave packet numerically.

Extensions of the above methods to general reactive systems are in principle fairly straightforward. For example, the extension to three-dimensional A + BC reactions is straightforward, with even a slight simplification due to the separability of final 2d states into a direct-product of diatomic vibrational and rotational states. We have implemented this approach for state-to-state calculations, however, with only limited success. The main difficulty is the requirement to use a grid that is significantly larger than the one needed to get initial state-resolved probabilities The larger grid is needed to describe the product rovibrational states accurately. Perhaps a generalization of the distorted wave packet approach of Gray and Balint-Kurti (described above) could be used to deal with this difficulty.

For general $J > 0$ calculations in the adiabatic rotation approximation, matrices of the rotational constants, A and $\bar{B}$ (symmetric top) or A, B, and C (asymmetric top) rotational constants would have to be calculated once in the $J = 0$ eigenbasis and then used exactly as described above to obtain the $J > 0$ eigenbasis. For an exact or CS calculation, the $J = 0$ eigenbasis would have to be augmented by the addition of $K > 0$ eigenbases, where K is the usual body-fixed rotational projection quantum number. However, as is well recognized the number of K states is typically much less than the range of J-values needed to get observables, e.g., cross sections and rate constants.

III. Application to the H_2 + CN ↔ H + HCN Reaction

For the test of the present method we chose the H_2 + CN ↔ H + HCN reaction. This reaction has been extensively studied theoretically using reduced dimensionality quantum dynamics methods.[37,46−49] Recently, full 6-dimensional calculations have been carried out by Light and Zhang[50] and by Zhu et al.[51] To facilitate comparison with earlier state-to-state probabilities computed for this reaction, we used the potential energy surface (PES) developed by Sun and Bowman.[37] The semiempirical PES of Sun and Bowman is based in part on ab initio calculations and has been used in calculations of reaction probabilities and the thermal rate constant (which was in good agreement with experiment).[49] This PES has a linear transition state (TS) with a barrier of 4.1 kcal/mol and exothermicity of 20.5 kcal/mol. Two doubly degenerate bending modes were incorporated into the PES via an adiabatic bending potential.[37] (Note that a more accurate PES has been recently developed by Horst et al.[52] and used in reduced dimensionality quantum calculations.[48])

TABLE 1: Parameters of the Wave Packet Propagation (Length in bohr)

	parameters
scattering coordinate, R_a, range	3.0−12.0
no. of grid points/PODVR points/basis functions in R_a	300/120/90
diatomic coordinate, r_a, range	1.0−11.0
no. of grid points/PODVR points/basis functions in r_a	300/80/60
diatomic coordinate, z_a, range	1.6−4.5
no. of grid points/PODVR points/basis functions in z_a	50/30/10
position of damping region/dividing surface in R_a	8.6/8.5
position of damping region/dividing surface in r_a	7.3/7.2
damping exponent, C_d	0.02
no. of 3D basis functions/eigenstates	5400/1300
backward 1D propagation up to $R_{b,\max}/R_{a,\max}$	16.0/24.0
wave packet position $R_{b,0}$ or $R_{a,0}$/and width α	9.0 or 8.0/0.2

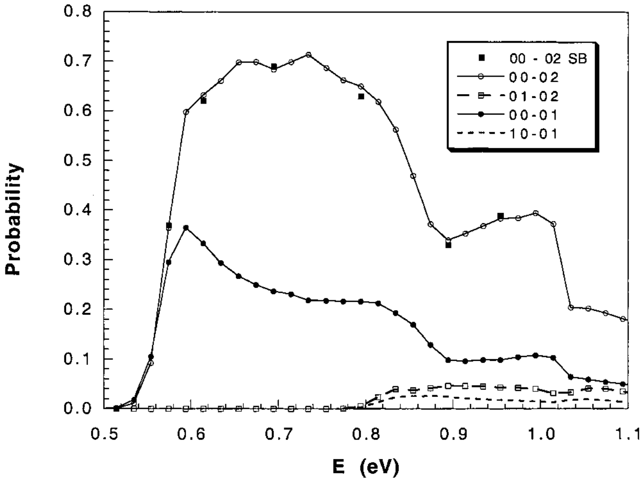

Figure 2. State-to-state probabilities for $H_2(0)$ + CN(0 or 1) ↔ H + HCN(v_s,v_a) reaction as a function of total energy. Final states are labeled by symmetric and asymmetric stretch quantum numbers of HCN. Also included are results from ref 45 (SB) for the 00 ↔ 02 transition.

The parameters of the calculation are given in Table 1, and the $J = 0$ state-to-state probabilities, for the ground adiabataic bend state, were computed for the ground vibrational state of H_2, the first two vibrational states of CN, and the first seven product states. The time step dt was chosen to be five atomic time units. Other parameters such as grid boundaries and basis set sizes were determined by numerous convergence tests of the one, two, and three degree-of-freedom bases used to obtain the L^2 eigenbasis.

Selected state-to-state reaction probabilities are shown in Figure 2. Reactant states are labeled by vibrational quantum numbers for H_2 and CN while product states are labeled by approximate quantum numbers: v_s, symmetric stretch of HCN, and v_a, asymmetric stretch of HCN. Excellent agreement, i.e., within a few percent, was found between the present results and earlier time-independent scattering calculations of Sun and Bowman (see Figure 4a in ref 37). We used 5400 basis functions to calculate $J = 0$ eigenstates while only 1300 eigenstates were used for propagation and also for the calculation of $J > 0$ eigenstates.

Probabilities for the (0,0) ↔ (0,2) transition are shown in Figure 3 as a function of the total energy for $J = 0$, 10, 20, 30,

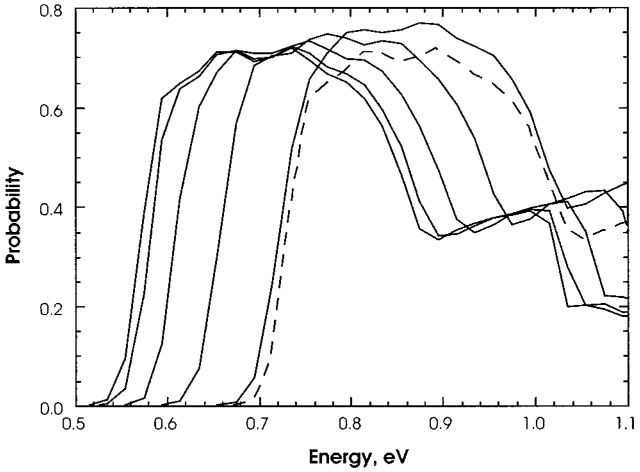

Figure 3. (0,0) ↔ (0,2) transition probabilities for $J = 0$, 10, 20, 30, and 40. Dashed line is the J-shifting result with $B = 0.777$ cm^{-1} for $J = 40$.

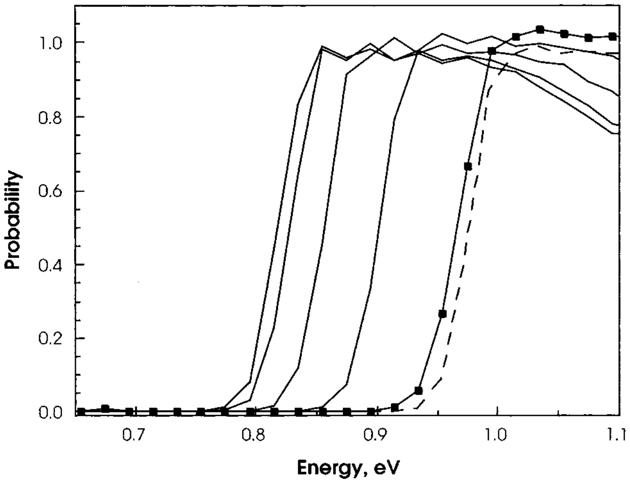

Figure 4. $H_2(0) + CN(1) \rightarrow H + HCN$ transition probabilities for $J = 0$, 10, 20, 30, and 40. Dashed line is the J-shifting result with $B = 0.777$ cm^{-1} for $J = 40$.

and 40. For comparison the $J = 40$ probability obtained from J-shifting, with the saddle point $\bar{B}$ constant of 0.78 cm^{-1}, is also shown. As seen, the adiabatic rotation approximation (ARA) results shift up to higher energies, in qualitative accord with J-shifting. Quantitatively there is very good agreement between the ARA and J-shifting probabilities. Note though that the J-shifting result is shifted to somewhat higher energies than the ARA one. This is probably due to some tunneling through the rotational barrier (which is 3.6 kcal/mol at the saddle point) in the ARA calculation.

Initial state-resolved reaction probabilities for $H_2(0)$ + CN(1) for $J = 0$, 10, 20, 30, and 40, and also the J-shifting result for $J = 40$ are shown in Figure 4. As seen, the ARA probabilities shift up in energy in the expected fashion, and the J-shifting result is in good agreement with the ARA one.

Another test of J-shifting that is relevant for rate constant calculations is for J-dependent cumulative reaction probabilities (for the ground bend state), $N_J(E)$. These probabilities are shown in Figure 5, and the comparison with the J-shifting approximation is made, again for $J = 40$. As seen there is good agreement with ARA result for $J = 40$; however, at higher energies the J-shifting result is roughly 15% below the ARA one.

To further investigate the accuracy of J-shifting we determined B-constants numerically from the ARA $N_J(E)$ probabilities as a function of J. The B-constants were determined by a simple fit procedure. The values determined range from 0.72 to 0.74 cm^{-1}, i.e., about 5−7% below rotational constant of the saddle point. (The reduction in the rotational constant relative to the value at the saddle point is almost certainly a signature that the variational transition state is located somewhat earlier in the reactant channel than the saddle point location.) This very good level of accuracy for J-shifting is probably due to the linear geometry of the saddle point, which results in a very simple description of the overall rotation.

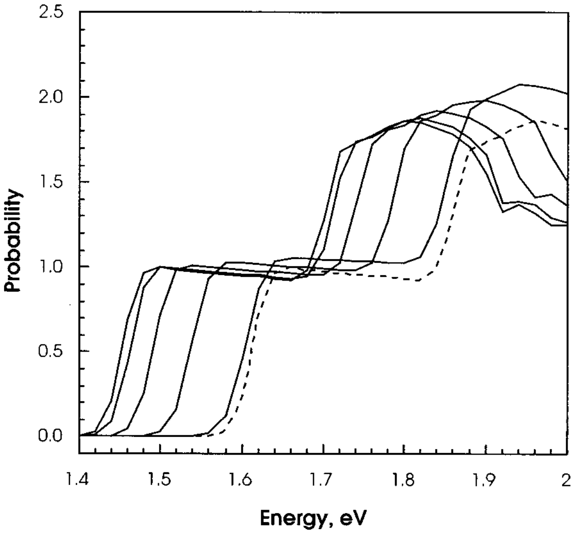

Figure 5. Cumulative reaction probabilities (for the ground bend state) for $J = 0$, 10, 20, 30, and 40. Dashed line is the J-shifting result with $B = 0.777$ cm^{-1} for $J = 40$.

Finally, we would like to mention other possible approximations for $J > 0$ calculations. Since the calculation of full **B**-matrix, eq 28, is somewhat involved, we have also tested first-order perturbation theory for propagation of $J > 0$ wave packets. Within this approach only diagonal elements of B_{ij} are required and eigenstates remain unchanged. Unfortunately, this simple approach underestimated the shift of $N_J(E)$ by about 30%, i.e., it is much less accurate than standard J-shifting. In another approximation, we computed the **B**-matrix within the CS approximation; this simplifies the calculation of B_{ij} because the CS B-constant depends on R_a only. This approach was also found to be inaccurate. Indeed, the TS rotational constant within the CS approximation is overestimated by about 70%; 1.34 cm^{-1} as compared to ARA TS rotational constant of 0.78 cm^{-1}. As a result, the use of CS approximation for the **B**-matrix gave much larger shifts of $N_J(E)$. Finally we used AR approximation to compute diagonal B_{ii} elements and the CS approximation to compute off-diagonal elements. The rationale was that shift of probabilities is dominated by change in energies of TS states accurately captured by diagonal elements, while small off-diagonal elements should be less important. Yet, this approach is also not accurate and overestimates the shift of probabilities by about 20%.

IV. Summary

We presented a wave packet propagation method based on real L^2 eigenstates, with damping, for reduced dimensionality/adiabatic bend AB + CD reactions, with CD treated as a spectator mode. In this approach, the wave packet is expanded in the basis of eigenstates and propagated by explicit time evolution of expansion coefficients with damping of the wave packet at each time step. The calculation of eigenstates represents the most difficult and time-consuming part of this approach. Yet, if eigenstates can be obtained, the wave packets for many initial states can be propagated very efficiently.

For the calculation of state-to-state reaction probabilities, the initial wave packet is expressed in product coordinates, transformed into reactant coordinates, and then expanded in terms of L^2 eigenstates in reactant coordinates. The coordinate transformation needs to be done only once for each initial wave packet, and due to the use of underlying analytical bases, the transformation is fast and simple. State-to state probabilities are computed by projecting reactive flux onto the initial reactant states along a dividing surface in reactant coordinates.

State-to-state probabilities computed for the collinearly dominated $H_2 + CN$ reaction, in reduced dimensionality, for zero total angular momentum were found to be in very good agreement with results obtained earlier on the same PES within a time-independent approach.

We also showed that eigenstates computed for $J = 0$ can be used for an efficient calculation of the eigenbasis for $J > 0$, within the adiabatic rotation approximation. The approach is based on the fact that $J = 0$ eigenstates represent a suitable and very compact basis for calculation of $J > 0$ eigenstates. Thus $J > 0$ eigenstates can be obtained for only a fraction of CPU cost required for $J = 0$ eigenstates. The simple J-shifting approximation was found to be quite accurate for the present system. We anticipate, however, that the current approach for $J > 0$ calculations will be very useful for more challenging systems. In particular, for barrierless reactions and reactions with nonlinear TS, the J-shifting is expected to be much less accurate and exact $J > 0$ calculations might be unavoidable.

Acknowledgment. This work was supported by the Department of Energy under the grant DE-FG02-97ER14782. We thank Stephen Gray for helpful discussions.

References and Notes

(1) Zhang, D. H.; Zhang, J. Z. H. In *Dynamics of Molecular and Chemical Reactions*; Wyatt, R. E., Zhang, J. Z. H., Eds.; Marcel Dekker: New York, 1996; Chapter 6.

(2) Kosloff, R. Chapter 5. In *Dynamics of Molecular and Chemical Reactions*; Wyatt, R. E., Zhang, J. Z. H., Eds.; Marcel Dekker: New York, 1996.

(3) Feit, M. D.; Fleck, J. A.; Steinger, A. *J. Comput. Phys.* **1982**, *47*, 412.

(4) Tal-Ezer, H.; Kosloff, R. *J. Chem. Phys.* **1984**, *81*, 3967.

(5) Leforestier, C.; Wyatt, R. E. *J. Chem. Phys.* **1983**, *78*, 2334.

(6) Neuhauser, D.; Judson, R. S.; Baer, M.; Kouri, D. Time-dependent wave packet approach to reactive scattering using arrangment decoupling absorbing potentials. In *Advances in molecular vibrations and collision dynamics*; JAI Press: Greenwich: CT, 1994; Vol. 2B, p 27.

(7) Kosloff, R.; Kosloff, D. *J. Comput. Phys.* **1986**, *63*, 363.

(8) Chen, R.; Guo, H. *J. Chem. Phys.* **1996**, *105*, 3569.

(9) Gray, S. K.; Balint-Kurti, G. G. *J. Chem. Phys.* **1998**, *108*, 950.

(10) Heather, R.; Metiu, H. *J. Chem. Phys.* **1987**, *86*, 5009.

(11) Das, S.; Tannor, D. J. *J. Chem. Phys.* **1990**, *92*, 3403.

(12) Zhang, J. Z. H. *Chem. Phys. Lett.* **1989**, *160*, 417.

(13) Zhang, J. Z. H. *J. Chem. Phys.* **1990**, *92*, 324.

(14) Zhang, D. H.; Sharafeddin, O. A.; Zhang, J. Z. H. *Chem. Phys.* **1992**, *167*, 137.

(15) Gogtas, F.; Balint-Kurti, G. G.; Offer, A. R. *J. Chem. Phys.* **1996**, *104*, 7927.

(16) Judson, R. S.; Kouri, D. J.; Neuhauser, D.; Baer, M. *Phys. Rev. A* **1990**, *42*, 351.

(17) Zhu, W.; Peng, T.; Zhang, J. Z. H. *J. Chem. Phys.* **1996**, *106*, 1742.

(18) Althorpe, S. C.; Kouri, D. J.; Hoffman, D. K. *J. Chem. Phys.* **1997**, *A42*, 351.

(19) Bowman, J. M. *J. Chem. Phys.* **1991**, *95*, 4960.

(20) Mielke, S. L.; Lynch, G. C.; Truhlar, D. G.; Schwenke, D. W. *J. Phys. Chem.* **1994**, *98*, 8000.

(21) Chatfield, D. C.; Mielke, S. L.; Allison, T. C.; Truhlar, D. G. *J. Chem. Phys.* **2000**, *112*, 8000.

(22) Zhang, D. H.; Zhang, J. Z. H. *J. Chem. Phys.* **1999**, *110*, 7622.

(23) Bowman, J. M.; Shnider, H. *J. Chem. Phys.* **1999**, *110*, 4428.

(24) Nobusada, K.; Nakamura, H. *J. Chem. Phys.* **1999**, *103A*, 6715.

(25) Matzkies, F.; Manthe, U. *J. Chem. Phys.* **2000**, *110*, 4428.

(26) Thompson, W.; Miller, W. H. *J. Chem. Phys.* **1997**, *106*, 142.

(27) Gray, S. K.; Goldfield, E. M.; Schatz, G. C.; Balint-Kurti, G. G. *Phys. Chem. Chem. Phys.* **1999**, *1*, 1141.

(28) (a) Bittererova, M.; Bowman, J. M. *J. Chem. Phys.* **2000**, *113*. (b) Bittererova, M.; Bowman, J.; Peterson, K. *J. Chem. Phys.* Submitted for publication.

(29) Pack, R. T. *J. Chem. Phys.* **1974**, *60*, 633.

(30) McGuire, P.; Kouri, D. J. *J. Chem. Phys.* **1974**, *60*, 2488.

(31) Bowman, J. M. *Chem. Phys. Lett.* **1994**, *217*, 36. (b) Wang, D.; Bowman, J. M. *J. Phys. Chem.* **1994**, *98*, 7994.

(32) McCurdy, C. W.; Miller, W. H. ARA Approximation. In *ACS Symposium Series*; Brooks, P. R., Hayes, E. F., Eds.; American Chemical Society: Washington, DC, 1977; Vol. 56, p 239.

(33) DeFazio, D.; Castillo, J. F. *Phys. Chem. Chem. Phys.* **1999**, *1*, 1165.

(34) Skokov, S.; Bowman, J. M. *Phys. Chem. Chem. Phys.* **2000**, *2*, 495.

(35) Skokov, S.; Tsuchida, T.; Nanbu, S.; Bowman, J. M.; Gray, S. K. *J. Chem. Phys.* **2000**, *113*, 227.

(36) Skokov, S.; Bowman, J. M. *J. Chem. Phys.* **2000**, *113*, 779.

(37) Sun, Q.; Bowman, J. M. *J. Chem. Phys.* **1990**, *92*, 5201.

(38) Sun, Q.; Bowman, J. M. *Int. J. Quantum Chem.* **1989**, *23*, 115.

(39) Skokov, S.; Qi, J.; Bowman, J. M.; Yang, C.-Y.; Gray, S. K.; Peterson, K. A.; Mandelshtam, V. A. *J. Chem. Phys.* **1998**, *109*, 10273.

(40) Colbert, D. T.; Miller, W. H. *J. Chem. Phys.* **1991**, *96*, 1982.

(41) Echave, J.; Clary, D. C. *Chem. Phys. Lett.* **1992**, *190*, 225.

(42) Zhang, D. H.; Zhang, J. Z. H. *J. Chem. Phys.* **1994**, *101*, 1146.

(43) Neuhauser, D. *Chem. Phys. Lett.* **1992**, *200*, 173.

(44) Meijer, J. H. M.; Goldfield, E. M.; Gray, S. K.; Balint-Kurti, G. G. *Chem. Phys. Lett.* **1998**, *293*, 270.

(45) Sun, Q.; Bowman, J. M. *J. Chem. Phys.* **1990**, *92*, 1021.

(46) Brooks, A. N.; Clary, D. C. *J. Chem. Phys.* **1990**, *92*, 4178.

(47) Clary, D. C. *J. Phys. Chem.* **1995**, *99*, 13664.

(48) Takayanagi, T.; Schatz, G. C. *J. Chem. Phys.* **1997**, *106*, 3227.

(49) Sun, Q.; Yang, D. L.; Wang, N. S.; Bowman, J. M.; Lin, M. C. *J. Chem. Phys.* **1990**, *93*, 4730.

(50) Light, J. C.; Zhang, D. H. *Faraday Discuss.* **1998**, *110*, 105.

(51) Zhu, W.; Zhang, J. Z. H.; Zhang, Y. C.; Zhang, Y. B.; Zhang, L. X.; Zhang, S. L. *J. Chem. Phys.* **1998**, *108*, 3509.

(52) terHorst, M. A.; Schatz, G. C.; Harding, L. B. *J. Chem. Phys.* **1996**, *105*, 2309.